Supporting Information

Sadakata et al. 10.1073/pnas.1210055109

SI Materials and Methods

Antibodies. The following primary antibodies were used for Western blotting: guinea pig polyclonal anti-Ca^{2+}-dependent activator protein for secretion 2 (Caps2) (1:10,000 dilution) (1) and mouse monoclonal antiactin (1:500 dilution; A4700; Sigma-Aldrich). The following primary antibodies were used for immunohistochemistry and immunocytochemistry: guinea pig polyclonal anti-Ca^{2+}-Caps2 (1:5,000 dilution) (1), rabbit polyclonal anti–brain-derived neurotrophic factor (BDNF) (1:100 dilution) (2), rabbit polyclonal anti-green fluorescent protein (GFP) (1:400 dilution; A11122; Life Technologies), anti-MAP2(a+b) (1:1,000 dilution; M1406; Sigma-Aldrich), mouse monoclonal anti-parvalbumin (1:4,000 dilution; P3088; Sigma-Aldrich), mouse monoclonal anti-Tau (1:300 dilution; 610672; BD Biosciences), rabbit polyclonal antisynaptophysin (1:100 dilution; RB-1461-P0; Thermo Scientific), and rabbit polyclonal anticalbindin (1:1,000 dilution; AB1778; Millipore). A polyclonal antibody was raised against recombinant human BDNF (whole BDNF) in male New Zealand white rabbits (Japan SLC) (2). Purified anti-BDNF antibody was tested for specific reactivity with the antigen (recombinant human BDNF) but not with mouse nerve growth factor (NGF) or recombinant human neurotrophin-3 (NT-3) (2). It was also confirmed that the purified anti-BDNF antibody could immunoreact with specific areas of the hippocampus in wild-type mice but not in BDNF-knockout mice (3).

Generation of Caps2 Exon 3-Skipped Mice. After transfecting MS12 embryonic stem (ES) cells (a C57BL/6 mouse ES cell line) (4) by electroporation, targeted clones were screened for G418 resistance with the targeting vector and analyzed by Southern blotting. Chimeric mice were generated by injection of targeted MS12 ES cells into mouse BALB/c blastocysts; the chimeras were mated with wild-type C57BL/6J mice to obtain heterozygous mutant mice. All of the engineered animals studied were backcrossed with C57BL/6J mice for more than five generations.

Immunohistochemistry. C57BL/6J male mice were killed by anesthesia with diethyl ether. Mice were transcardially perfused, initially with PBS and then with Zamboni's fixative [2% (wt/vol) paraformaldehyde in 0.1 M phosphate buffer, pH 7.4, containing 0.2% picric acid]. Tissues were dissected, postfixed in Zamboni's fixative at 4 °C for 5 h, and cryoprotected by immersion in 15% (wt/vol) sucrose in PBS overnight at 4 °C. After embedding in Tissue-Tek OCT compound (Sakura Finetechnical), tissues were frozen in dry ice powder, and sectioned at a thickness of 14 μm using a cryostat (CM1850; Leica Microsystems) at −18 °C. The sections were air dried for 1 h and rinsed three times in PBS. After blocking with 5% (wt/vol) BSA and 0.3% Triton X-100 in PBS at room temperature (RT) for 1 h, the sections were reacted at 4 °C overnight with primary antibody in an immunoreaction buffer [2× PBS containing 0.3% Triton X-100 and 1% (wt/vol) BSA], rinsed in PBS, and then reacted at RT for 1 h with secondary antibody in the same immunoreaction buffer, and rinsed again in PBS. Immunoreacted sections were mounted with Vectashield mounting medium (Vector Laboratories) and observed using a microscope (BX51; Olympus) equipped with a charge-coupled device (CCD) camera (VB-7000; Keyence). Digital images were processed using Adobe Photoshop 6.0 software (Adobe Systems).

Immunocytochemistry. Cells were fixed with Zamboni's fixative at RT for 15 min. After washing three times with PBS, cells were permeabilized in PBS containing 0.02% Triton X-100 at RT for 5 min. After blocking with Image-iT FX signal enhancer (Invitrogen) at RT for 60 min, cells were incubated with primary antibodies at 4 °C overnight, rinsed in PBS, then incubated with Alexa-conjugated secondary antibodies (1:1,000 dilution; Invitrogen) at RT for 1 h, and again rinsed in PBS. Immunoreacted cells were mounted with Vectashield mounting medium (Vector Laboratories). Images were acquired with a microscope (BX51; Olympus) equipped with a CCD camera (VB-7000; Keyence). Digital images were processed using Adobe Photoshop 6.0 software (Adobe Systems).

Primary Cultures of Hippocampal Granule Cells. Primary-cultured hippocampal granule cells from mice were prepared using previously described methods (5), with slight modifications. Briefly, three-day-old C57BL/6J mice (Nippon SLC) were deeply anesthetized by ether, and the hippocampal formation was immediately dissected and placed in ice-cold Gey's balanced salt solution bubbled with a gas mixture of 95% O_2 and 5% CO_2. After removal of the subicular complex along the sulcus hippocampi, the remaining part was divided into the dentate gyrus and Ammon's horn. Both tissues were cut into pieces and treated with 0.25% trypsin (Difco Laboratories) and 0.01% DNase I (Sigma-Aldrich) at 37 °C for 30 min. The incubation was terminated by the addition of heat-inactivated horse serum. The tissue fragments were centrifuged at 250 × *g* for 5 min, the supernatant was removed, and the pellet was resuspended in a mixture of 50% Neurobasal/B-27 and 50% astrocyte-conditioned medium. The cells were plated at a density of 5.0×10^4 cells/cm^2 onto poly-L-lysine–coated cell culture plates. To prevent proliferation of glial cells, the culture medium was changed to conditioned medium-free neurobasal/B-27 medium supplemented with 2 μM cytosine-D-arabino-furanoside (Sigma-Aldrich) 24 h after plating. Half of the medium was exchanged every 3 d.

On days in vitro (DIV) 6, neurons were transfected with BDNF–GFP using Lipofectamine 2000 (Invitrogen). Twenty-four hours after transfection, cultured neurons were stimulated with medium containing various concentrations of KCl for 10 min, fixed with 4% (wt/vol) paraformaldehyde (PFA)/PBS, and then washed with PBS. After blocking with 5% (vol/vol) normal donkey serum/PBS (Vector Laboratories), cells were incubated with anti-GFP antibody at RT for 2 h, rinsed in PBS, permeabilized, incubated with anti-MAP2(a+b) antibody at RT for 2 h, rinsed in PBS, incubated with Alexa Fluor-conjugated secondary antibody at 4 °C overnight, and then rinsed in PBS. Immunoreacted cells were mounted with Vectashield mounting medium (Vector Laboratories). Images were acquired with a microscope (BX51; Olympus) equipped with a CCD camera (VB-7000; Keyence). Digital images were processed using Adobe Photoshop 6.0 software (Adobe Systems).

Behavioral Tests. Two-month-old male mice were used unless otherwise described. All mice used were the littermate progeny of intercrossed heterozygotes. The experimenter was blind to the genotype.

Rotarod testing. Rotarod testing was carried out as described previously (6) using a Rota-Rod Treadmill for Mice 7600 (Ugo Basile). All mice used in the experiments below were littermates from mated heterozygotes. Briefly, a male mouse was required to run backward to maintain its position on top of a rod revolving at 24 rpm. Each time it fell, the mouse was put back on the rod until it had run for a total of 3 min on the rod. The time was not

counted while the mouse was off the rod. The latency to first fall and the total number of falls within 3 min were recorded.

Grip traction test. Muscle strength was tested by a mouse's ability to hang on by its forepaws to a horizontal wire placed above the table. The time during which the mouse remained hanging was recorded (7).

Open-field test and novel object recognition test. The test was performed as previously described (8, 9) with minor modifications. Locomotor activity was measured in an open field (60 × 60 cm) at 50 lx (at the surface level of the area). Each mouse was placed in the center of the open field, and its horizontal movements were monitored for 15 min with a charge-coupled device camera. The images were processed with National Institutes of Health (NIH) Image Open Field (O.F.) software (O'Hara & Co.).

Social interaction test. The social interaction test was performed as previously described (8) with minor modifications. A vacant small cage was placed in the home cage with the subject for 24 h. Social interaction was measured in the open field apparatus described above. A small cage containing a stranger C57BL/6J mouse was placed in one corner. Each mouse was placed into the open field for 15 min.

Y-maze test. Spontaneous alternation to explore new environments was assessed to test spatial recognition memory as described previously (10). The acrylic symmetrical Y maze consists of three arms (40 × 3 cm) each separated by 120°, with 13-cm-high transparent walls (O'Hara & Co.). Each mouse (11–13 wk of age) was placed in the center of the Y maze and allowed to explore freely for 5 min. The sequence and total number of arms entered were recorded. The percentage of alternation is the number of triads containing entries into all three arms divided by the maximum possible number of alternations (total number of arm entries − 2) × 100.

Olfactory test. The hidden-cookie test was performed as previously described (11). Male mice (n = 9 of each genotype) were food deprived overnight. A piece of butter cookie (Morinaga, <0.7 g per piece) was buried beneath about 3 cm of clean bedding in a random location. The mouse was placed in the cage, again in a random location, during the light phase. The latency time to locate the cookie was recorded. We defined finding the cookie as when the mouse held it in both paws.

Elevated plus maze. The elevated plus maze was set at a height of 65 cm and consisted of four gray plexiglass arms, each 8-cm-wide × 25-cm-long with 15-cm-high walls. Two arms were open, and two were enclosed. Individual mice were placed in the center of the maze, and the total distance and time spent in each arm were measured, and analyzed with NIH Image Elevated Plus (E.P.) software (O'Hara & Co.).

Light/dark transition test. The light/dark transition test was performed as previously described (12). The apparatus consisted of a cage (40 × 20 × 20 cm) bisected by a black partition containing a small opening (O'Hara & Co.). One chamber was open and brightly illuminated, whereas the other chamber was closed and dark. Mice were placed into the dark side and allowed to move freely between the two chambers for 10 min. The time spent in the light side was recorded, and analyzed with NIH Image Light/Dark (L.D.) software (O'Hara & Co.).

Home-cage activity. Home-cage activity was measured as previously described (13). Spontaneous locomotor activity in the home cage (18 cm wide × 14 cm high × 32 cm deep) was determined by counting photobeam interruptions using SCANET (6 channel SV-20 system; Melquest) for 6 d, after 24 h habituation to a fresh cage. The distance between the sensors was 0.5 cm. Mice were housed individually under the 12-h light/dark cycle described above. Food and water were available ad libitum. The experiment was begun at 08:00, and lasted 3 d.

Neonate survival test. The mice used were 2-mo-old primiparous females. Wild-type females were mated with $Caps2^{\Delta ex3/\Delta ex3}$ males, and vice versa. Pregnant wild-type or $Caps2^{\Delta ex3/\Delta ex3}$ females were housed separately and were not touched for at least 5 d before giving birth.

Ultrasound vocalization test. Animals were assessed for ultrasound vocalization (USV) between P5 and P10. Wild-type females were mated with wild-type or $Caps2^{\Delta ex3/\Delta ex3}$ males. The pups were separated from their dam immediately before recording and were positioned in a sound-attenuating chamber below a condenser ultrasound microphone (40011; Avisoft Bioacoustics) to detect USVs at 50–100 kHz. The duration of calls was recorded and quantified with an Avisoft recorder (Avisoft Bioacoustics) during a 10-min test.

Recording of circadian rhythm. Circadian rhythm was recorded as previously described (14). Wheel running was measured with a wheel meter (WW-3302; O'Hara & Co.), which comprises a set of 20 rooms (14.3 cm wide × 14.8 cm high × 29.3 cm deep) containing a wheel cage (50 cm diameter × 5 cm wide). The mice were housed one per room, were able to move freely, and were given free access to food and water. Every 1/3 revolution of the wheel cage was recorded as one count. The circadian period was calculated using a χ^2 periodogram.

1. Sadakata T, Washida M, Morita N, Furuichi T (2007) Tissue distribution of Ca^{2+}-dependent activator protein for secretion family members CAPS1 and CAPS2 in mice. *J Histochem Cytochem* 55(3):301–311.
2. Katoh-Semba R, Takeuchi IK, Semba R, Kato K (1997) Distribution of brain-derived neurotrophic factor in rats and its changes with development in the brain. *J Neurochem* 69(1):34–42.
3. Katoh-Semba R, et al. (2001) Induction of brain-derived neurotrophic factor by convulsant drugs in the rat brain: Involvement of region-specific voltage-dependent calcium channels. *J Neurochem* 77(1):71–83.
4. Kawase E, et al. (1994) Strain difference in establishment of mouse embryonic stem (ES) cell lines. *Int J Dev Biol* 38(2):385–390.
5. Baba A, Yamada MK, Nishiyama N, Matsuki N, Ikegaya Y (2002) Different Ca^{2+} dynamics between isolated hippocampal pyramidal cells and dentate granule cells. *J Neurocytol* 31(1):41–48.
6. Lynch A, Smart JL, Dobbing J (1975) Motor co-ordination and cerebellar size in adult rats undernourished in early life. *Brain Res* 83(2):249–259.
7. Spandou E, et al. (2005) Erythropoietin prevents long-term sensorimotor deficits and brain injury following neonatal hypoxia-ischemia in rats. *Brain Res* 1045(1-2):22–30.
8. Tomemori Y, et al. (2005) A gene-targeted mouse model for chorea-acanthocytosis. *J Neurochem* 92(4):759–766.
9. Dulawa SC, Grandy DK, Low MJ, Paulus MP, Geyer MA (1999) Dopamine D4 receptor-knock-out mice exhibit reduced exploration of novel stimuli. *J Neurosci* 19(21):9550–9556.
10. Mishima K, et al. (2004) Characteristics of behavioral abnormalities in alpha1d-adrenoceptors deficient mice. *Behav Brain Res* 152(2):365–373.
11. Wersinger SR, Ginns EI, O'Carroll AM, Lolait SJ, Young WS, 3rd (2002) Vasopressin V1b receptor knockout reduces aggressive behavior in male mice. *Mol Psychiatry* 7(9): 975–984.
12. Miyakawa T, Yamada M, Duttaroy A, Wess J (2001) Hyperactivity and intact hippocampus-dependent learning in mice lacking the M1 muscarinic acetylcholine receptor. *J Neurosci* 21(14):5239–5250.
13. Ohdo S, Koyanagi S, Suyama H, Higuchi S, Aramaki H (2001) Changing the dosing schedule minimizes the disruptive effects of interferon on clock function. *Nat Med* 7(3):356–360.
14. Uchihashi Y, Kuribara H, Yasuda H, Umezu T, Tadokoro S (1994) Long-continuous observation of the effects of methamphetamine on wheel-running and drinking in mice. *Prog Neuropsychopharmacol Biol Psychiatry* 18(2):397–407.

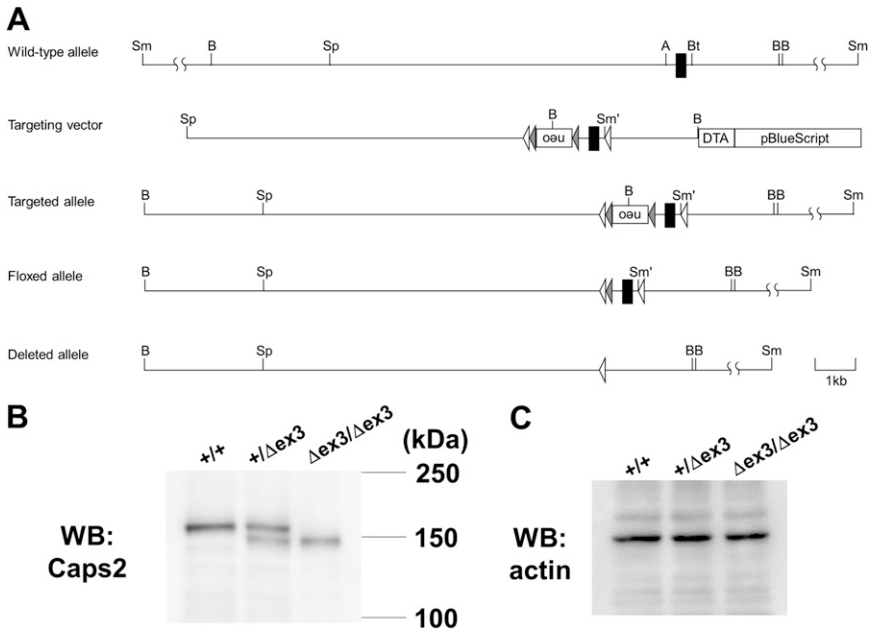

Fig. S1. Generation of *Caps2*$^{\Delta ex3/\Delta ex3}$ mice. (*A*) Maps of the mouse *Caps2* gene, the targeting vector, and the resultant targeted allele. The filled box denotes exon 3. Restriction enzyme sites: A, AatII; B, BamHI; Bt, BtrI; Sm, SmaI; and Sp, SpeI. DTA, diphtheria toxin fragment A. White triangles represent loxP sites, gray triangles represent FRT sites. (*B* and *C*) Immunoblot analysis of the cerebellum of P8 wild-type, *Caps2*$^{+/\Delta ex3}$, and *Caps2*$^{\Delta ex3/\Delta ex3}$ mice. Protein lysates from the cerebellum were Western blotted (WB) with an anti-Caps2 (*B*) and an antiactin antibody (*C*).

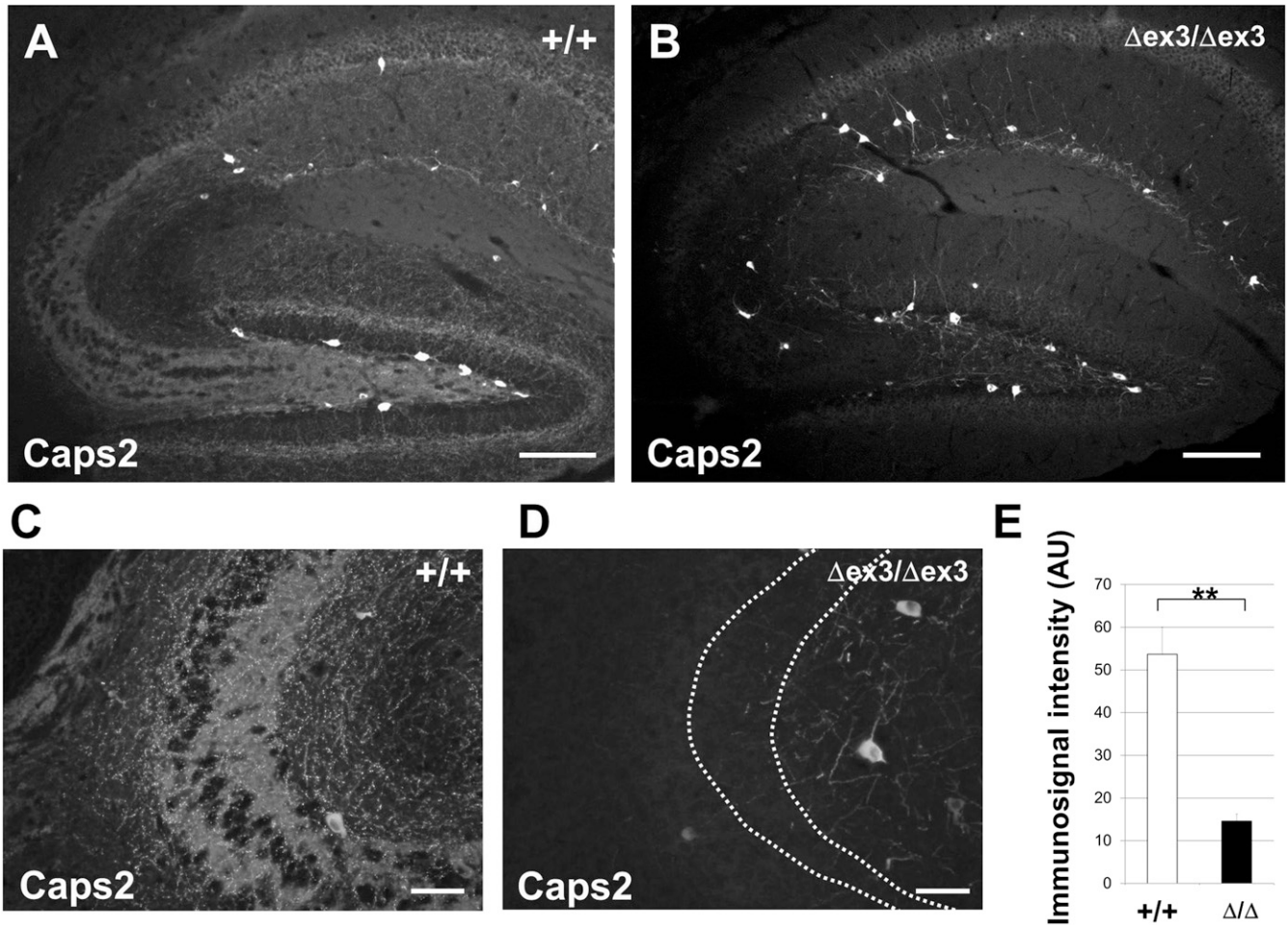

Fig. S2. Distribution of Caps2 protein in the *Caps2*$^{\Delta ex3/\Delta ex3}$ mouse hippocampus. (*A* and *B*) Sagittal sections of P21 wild-type (*A*) and *Caps2*$^{\Delta ex3/\Delta ex3}$ (*B*) hippocampus were immunolabeled with an anti-Caps2 antibody. (Scale bars, 100 μm.) (*C* and *D*) Sagittal sections of P21 wild-type (*C*) and *Caps2*$^{\Delta ex3/\Delta ex3}$ (*D*) hippocampal CA3 region were immunolabeled with an anti-Caps2 antibody. Dotted line indicates stratum lucidum. (Scale bars, 50 μm.) (*E*) Immunosignal intensities at stratum lucidum of wild-type (white bar) and *Caps2*$^{\Delta ex3/\Delta ex3}$ mice (black bar) are shown. Error bars indicate the SD $^{**}P < 0.01$, by Student *t* test.

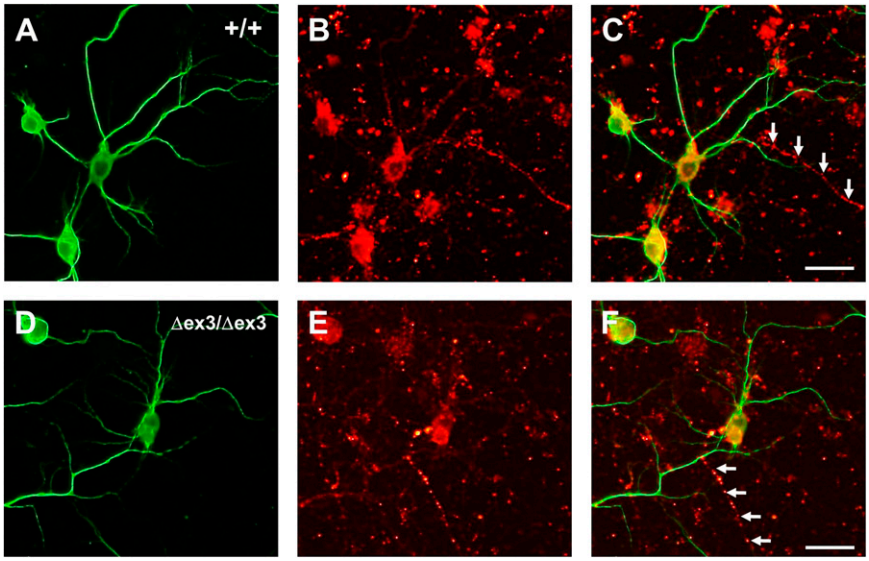

Fig. S3. Distribution of MAP2(a+b) and Tau in primary-cultured hippocampal cells. (*A*–*F*) Subcellular localization of MAP2(a+b) (*A* and *D*) and Tau (*B* and *E*) protein in wild-type (*A*–*C*) and *Caps2*$^{\Delta ex3/\Delta ex3}$ (*D*–*F*) hippocampal primary cultures immunostained for MAP2(a+b) (green) and Tau (red) at 14 d in vitro. Arrows show the position of the axon. Merged image is shown in *C* and *F*. (Scale bars, 30 μm.)

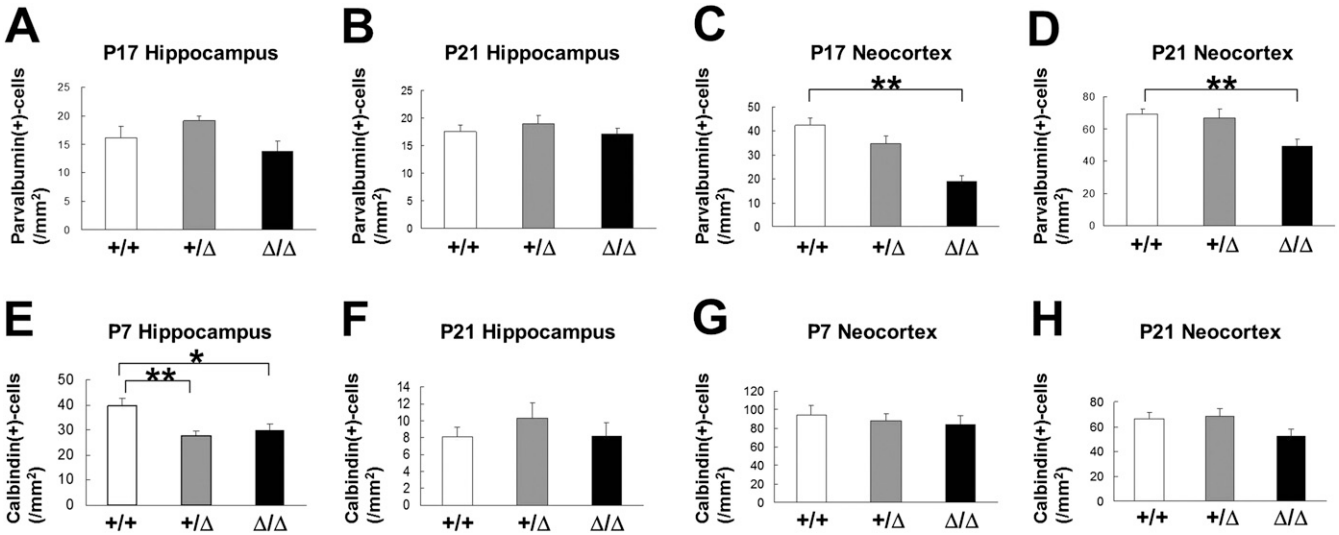

Fig. S4. Reduction in parvalbumin- and calbindin-positive cells in the hippocampus and neocortex of *Caps2*$^{\Delta ex3/\Delta ex3}$ mice during postnatal development. (*A–H*) Cell densities of parvalbumin-positive neurons (*A–D*) and calbindin-positive neurons (*E–H*) for wild-type (white), *Caps2*$^{+/\Delta ex3}$ (gray), and *Caps2*$^{\Delta ex3/\Delta ex3}$ (black) mice. (*A*) P17 hippocampus (n = 16, 19, and 14, respectively). (*B*) P21 hippocampus (n = 12, 16, and 16, respectively). (*C*) P17 neocortex (layers I–VI) (n = 14 for each) ($P < 0.01$, one-factor ANOVA). (*D*) P21 neocortex (layers I–VI) (n = 12, 16, and 16, respectively) ($P < 0.01$, one-factor ANOVA). (*E*) P7 hippocampus (n = 9, 18, and 12, respectively) ($P < 0.01$, one-factor ANOVA). (*F*) P21 hippocampus (n = 6, 6, and 8, respectively). (*G*) P7 neocortex (layers II–V) (n = 9, 8, and 12, respectively). (*H*) P21 neocortex (layers IV–V) (n = 8, 9, and 11, respectively). Error bars indicate SEM. *$P < 0.05$; **$P < 0.01$, by post hoc t test.

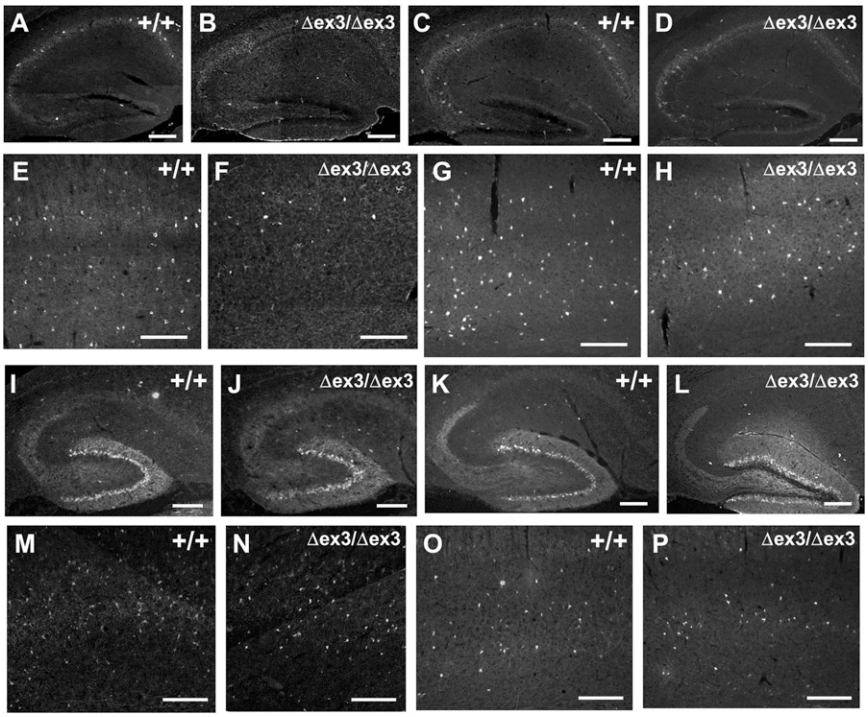

Fig. S5. Differences in the parvalbumin- and calbindin-immunostaining patterns in the hippocampus and neocortex between wild-type and *Caps2*$^{\Delta ex3/\Delta ex3}$ mice. (*A–H*) Sagittal sections of hippocampus (*A–D*) and neocortex (*E–H*) were immunolabeled with antiparvalbumin antibody. (*A* and *E*) Wild type at P17; (*B* and *F*) *Caps2*$^{\Delta ex3/\Delta ex3}$ at P17; (*C* and *G*) wild-type at P21; and (*F* and *H*) *Caps2*$^{\Delta ex3/\Delta ex3}$ at P21. (Scale bars, 200 μm.) (*I–P*) Sagittal sections of hippocampus (*I–L*) and neocortex (*M–P*) were immunolabeled with anticalbindin antibody. (*I* and *M*) Wild type at P7; (*J* and *N*) *Caps2*$^{\Delta ex3/\Delta ex3}$ at P7; (*K* and *O*) wild-type at P21; and (*L* and *P*) *Caps2*$^{\Delta ex3/\Delta ex3}$ at P21. (Scale bars, 200 μm.)

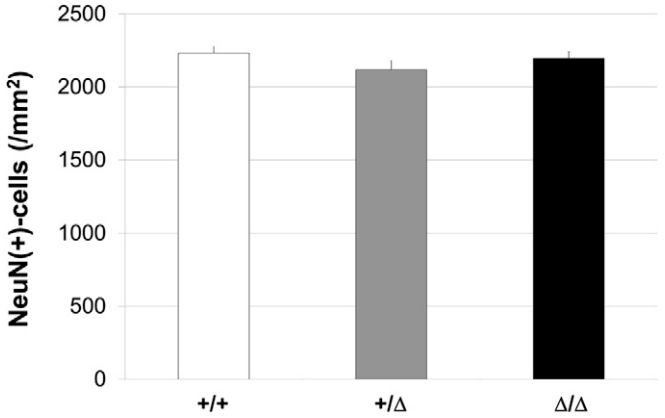

Fig. S6. Unchanged NeuN-positive neuronal density in the neocortex of *Caps2*$^{\Delta ex3/\Delta ex3}$ mice compared with wild-type mice. Cell densities of NeuN-positive neurons for wild-type (white), *Caps2*$^{+/\Delta ex3}$ (gray), and *Caps2*$^{\Delta ex3/\Delta ex3}$ (black) mice in the P21 neocortex (layers II–VI) (n = 8, 8, and 8, respectively). Error bars indicate SEM.

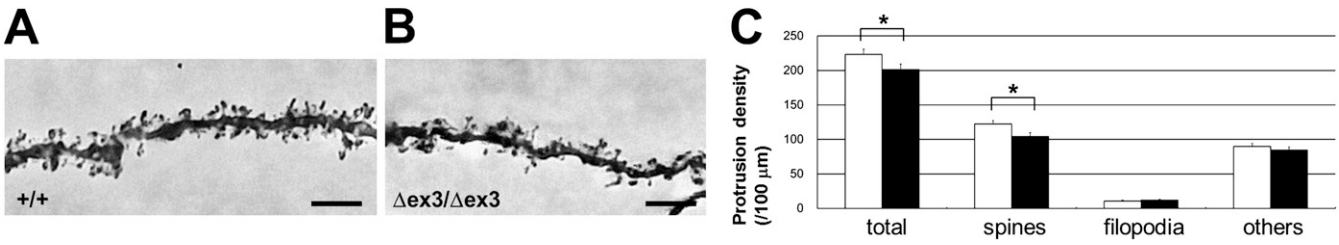

Fig. S7. Decreased dendritic spine density of granule cells in the hippocampal dentate gyrus of *Caps2*$^{\Delta ex3/\Delta ex3}$ mice. (*A* and *B*) Representative Golgi staining of a granule cell dendrite of the dentate gyrus from wild-type (*A*) and *Caps2*$^{\Delta ex3/\Delta ex3}$ (*B*) mice at P21. (Scale bars, 5 μm.) (*C*) Protrusion density of primary and secondary dendrites in dentate gyrus granule cells at P21 in wild-type (white; n = 26 from 12 mice) and *Caps2*$^{\Delta ex3/\Delta ex3}$ (black; n = 26 from 13 mice) littermates. Error bars indicate SEM. *$P < 0.05$, by Student t test.

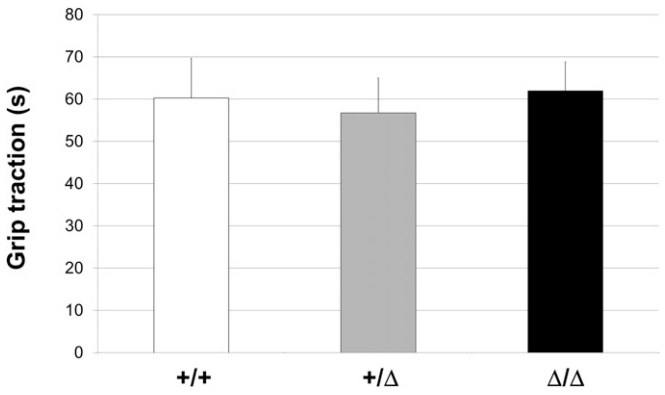

Fig. S8. Grip traction test. Time during which the mice remained hanging from a horizontal wire is presented for wild-type (white; n = 9), *Caps2*$^{+/\Delta ex3}$ (gray; n = 9), and *Caps2*$^{\Delta ex3/\Delta ex3}$ (black; n = 9) mice. Error bars indicate SEM.

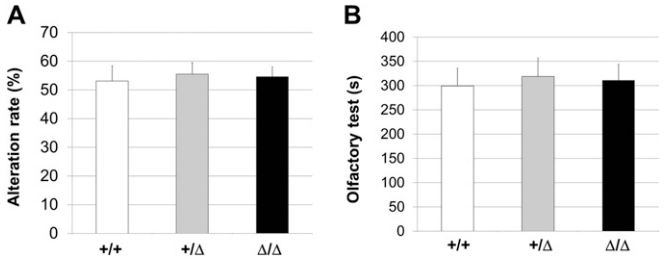

Fig. S9. Y-maze test and olfactory test. (*A*) Percentage correct alternation response in the Y-maze test is shown for wild-type (white; $n = 9$), *Caps2*$^{+/\Delta ex3}$ (gray; $n = 9$), and *Caps2*$^{\Delta ex3/\Delta ex3}$ (black; $n = 9$) mice. (*B*) Latency to locate a piece of cookie was recorded. We defined finding the cookie as when the mouse held it in both paws. No significant differences were observed among wild-type, *Caps2*$^{+/\Delta ex3}$, and *Caps2*$^{\Delta ex3/\Delta ex3}$ mice in these tests.

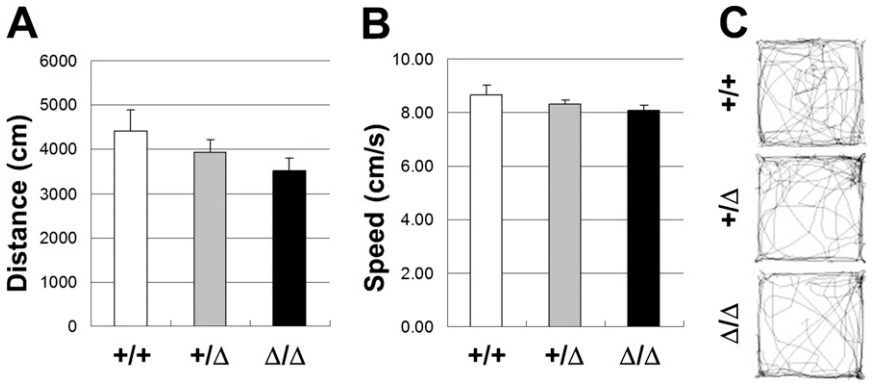

Fig. S10. Open-field test. (*A*–*C*) Horizontal movement distance (*A*) and speed (*B*) of an open field (15 min) are shown for wild-type (white; $n = 11$), *Caps2*$^{+/\Delta ex3}$ (gray; $n = 13$), and *Caps2*$^{\Delta ex3/\Delta ex3}$ (black; $n = 12$) mice. Representative movement traces are shown in *C*. Error bars indicate SEM.

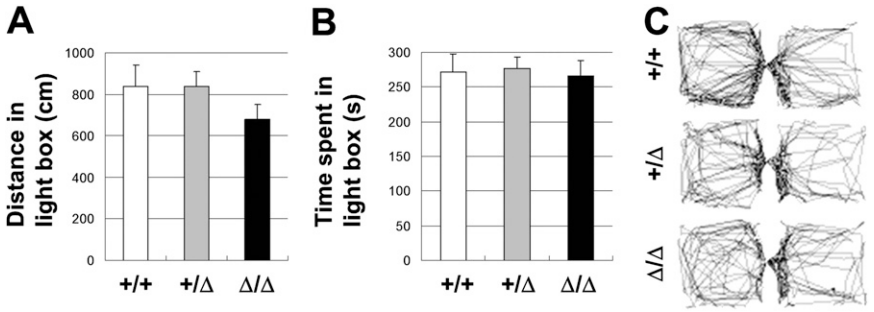

Fig. S11. Light/dark box test. (*A*–*C*) Horizontal movement distance in the light box (*A*) and time spent in the light box (*B*) of a light/dark box (10 min) is shown for wild-type (white; $n = 11$), *Caps2*$^{+/\Delta ex3}$ (gray; $n = 13$), and *Caps2*$^{\Delta ex3/\Delta ex3}$ (black; $n = 12$) mice. Representative movement traces are shown in *C*. Error bars indicate SEM.

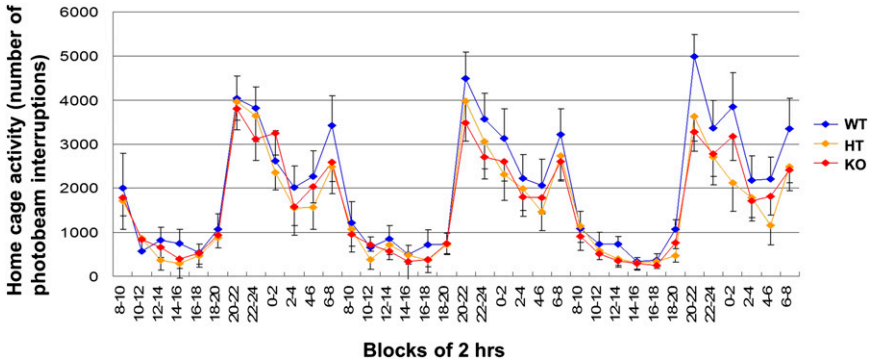

Fig. S12. *Caps2*$^{\Delta ex3/\Delta ex3}$ mice display impaired habituation to a fresh cage. After habituation to a fresh cage for 24 h, the locomotor activity of wild-type (blue; $n = 11$), *Caps2*$^{+/\Delta ex3}$ (orange; $n = 13$), and *Caps2*$^{\Delta ex3/\Delta ex3}$ (red; $n = 12$) mice was measured for 3 d (12-h light/dark period). Graph shows mean number of photobeam interruptions per 2 h. Error bars indicate SEM.

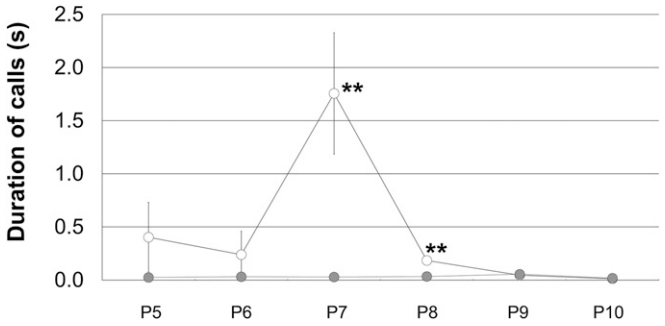

Fig. S13. Average duration of USVs per pup was reduced in *Caps2*$^{+/\Delta ex3}$ mice compared with wild-type mice. Wild-type females were mated with wild-type or *Caps2*$^{\Delta ex3/\Delta ex3}$ males. The developmental change in USVs is shown for wild-type (open circles; $n = 7$ litters) and *Caps2*$^{+/\Delta ex3}$ (gray circles; $n = 8$ litters) pups. Error bars indicate SEM. $P < 0.01$, repeated measures ANOVA. *$P < 0.05$; **$P < 0.01$, by post hoc *u* test.

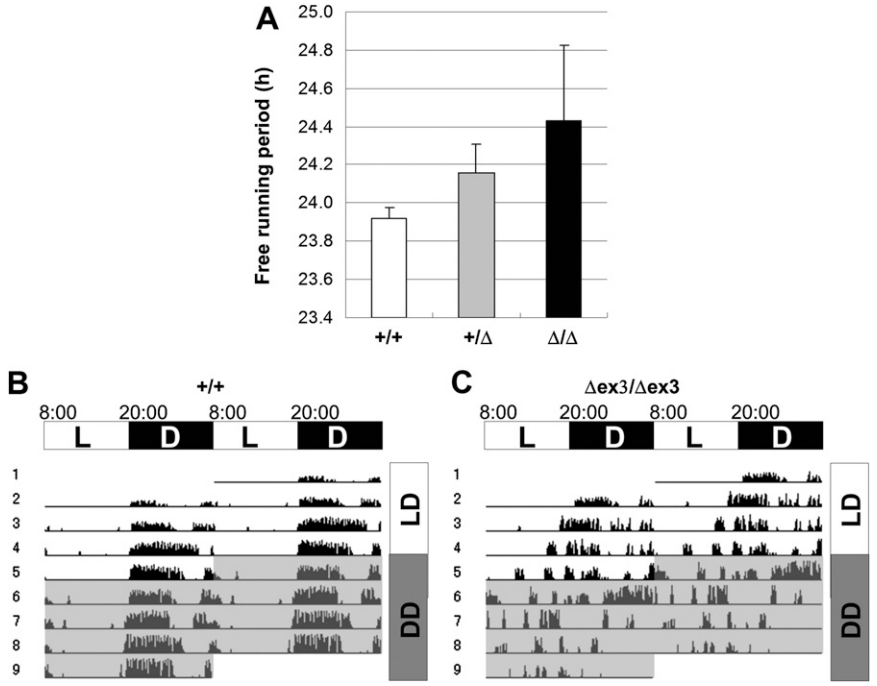

Fig. S14. Circadian rhythm of *Caps2*$^{\Delta ex3/\Delta ex3}$ mice. (*A*) Sleep–wake rhythms of locomotor activity under free wheel-running conditions in a constant dark cycle. Graph shows the circadian period (h) calculated by a χ^2 periodogram for wild-type (white; $n = 20$), *Caps2*$^{+/\Delta ex3}$ (gray; $n = 25$), and *Caps2*$^{\Delta ex3/\Delta ex3}$ (black; $n = 14$) mice. Error bars indicate SEM. (*B* and *C*) Light–dark rhythms of locomotor activity under free wheel-running conditions under a 12-h light/dark cycle (LD) and a constant dark cycle (DD). Activity traces for wild-type (*B*) and *Caps2*$^{\Delta ex3/\Delta ex3}$ (*C*) mice for 4 d of light/dark cycle and 4 d of constant darkness are represented as relative deflections from the horizontal line. Actograms are double-plotted over a 48-h period.